Efficient Calculation of Schwarz–Christoffel Transformations for Multiply Connected Domains Using Laurent Series

Thomas K. DeLillo, Alan R. Elcrat, Everett H. Kropf & John A. Pfaltzgraff

Computational Methods and Function Theory

ISSN 1617-9447
Volume 13
Number 2

Comput. Methods Funct. Theory (2013)
13:307-336
DOI 10.1007/s40315-013-0023-1

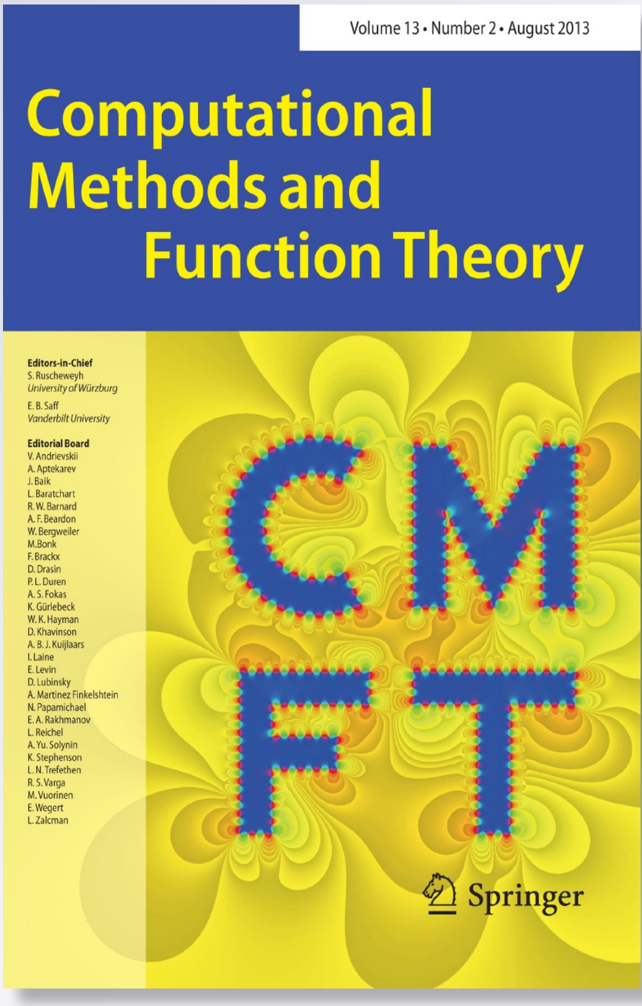

Springer

Comput. Methods Funct. Theory (2013) 13:307–336
DOI 10.1007/s40315-013-0023-1

Efficient Calculation of Schwarz–Christoffel Transformations for Multiply Connected Domains Using Laurent Series

Thomas K. DeLillo · Alan R. Elcrat · Everett H. Kropf · John A. Pfaltzgraff

Received: 21 September 2012 / Revised: 24 May 2013 / Accepted: 26 May 2013 / Published online: 25 June 2013

Abstract We discuss recently developed numerics for the Schwarz–Christoffel transformation for unbounded multiply connected domains. The original infinite product representation for the derivative of the mapping function is replaced by a finite factorization where the inner factors satisfy certain boundary conditions derived here. Least squares approximations based on Laurent series are used to satisfy the boundary conditions. This results in a much more efficient method than the original method based on reflections making the accurate mapping of domains of higher connectivity feasible.

The contributions of the third author were carried out as part of his PhD dissertation [15].

Dedicated to Nicolas Papamichael

Communicated by Lloyd N. Trefethen.

T. K. DeLillo (✉) · A. R. Elcrat
Department of Mathematics, Statistics, and Physics, Wichita State University,
Wichita, KS 67260-0033, USA
e-mail: delillo@math.wichita.edu

A. R. Elcrat
e-mail: elcrat@math.wichita.edu

E. H. Kropf
Department of Mathematics, Harvard University, Cambridge, MA 02138, USA
e-mail: ehkropf@gmail.com

J. A. Pfaltzgraff
Department of Mathematics, University of North Carolina, Chapel Hill, NC 27599, USA
e-mail: jap3658@hotmail.com

Keywords Schwarz–Christoffel transformation · Conformal mapping · Multiply connected domains · Laurent series

Mathematics Subject Classification (2000) Primary 30C30; Secondary 65E05

1 Introduction

In this paper we present recent work on an alternate representation and computation of the Schwarz–Christoffel transformations for multiply connected domains given in [8]. The transformations were based on infinite sequences of iterated reflections, which generated infinite products in each mapping formula. We will only discuss the unbounded case here.

The unbounded polygonal domain mapping is given in [8] by the formula

$$f(z) = A \int^{z} \prod_{j=1}^{m} \prod_{k=1}^{K_j} \left[\prod_{\substack{n=0 \\ \nu \in \sigma_n(j)}}^{\infty} \left(\frac{\zeta - z_{k,\nu j}}{\zeta - s_{\nu j}} \right) \right]^{\beta_{k,j}} \mathrm{d}\zeta + B. \tag{1}$$

Here, f is the conformal map $f : \Omega \to \mathbb{P}$ from the domain Ω exterior to m non-overlapping circles, C_j, $j = 1, \ldots, m$ with centers $c_j = s_j$ and radii r_j, to the domain $\mathbb{P}$ exterior to m bounded, mutually exterior polygons, $\Gamma_j = f(C_j)$. The kth prevertex $z_{k,j} \in C_j$, $k = 1, \ldots, K_j$, maps to the kth corner on the jth polygon, $w_{k,j} = f(z_{k,j}) \in \Gamma_j$. Also $f(\infty) = \infty$. The exponents $\beta_{k,j}\pi$ are the turning angles at the vertices of $\partial\mathbb{P}$ with $\sum_{k=1}^{K_j} \beta_{k,j} = 2$ for any fixed j. The boundaries of the circle and polygon domains are oriented such that the domain is to the right as one traces the boundary. The $z_{k,\nu j}$ are generated by reflections of the prevertex points on $\partial\Omega$. The $s_{\nu j}$ are generated by the point at infinity and its reflections.

Convergence of infinite products was proven in [8] for cases where the circles are sufficiently well-separated. In [10,15], a numerical method was developed for computing the maps for both bounded and unbounded domains based on truncating the infinite products and the sufficient conditions for convergence were found to be far from necessary, in practice. There do not appear to be any simple conditions which are both necessary and sufficient for convergence. Indeed, examples of non-convergence can be constructed for the equivalent Poincare series, and for practical computations with m much greater than about 3 or 4 the geometric increase in the number of terms with each level of reflection renders the formula impractical. Therefore, for both theoretical and computational reasons, it is desirable to have a formula for general domains in terms of more elementary functions which are always defined and may be more easily computed. In this paper, we develop such a more efficient approach. We show that the inner infinite products in the integrand of (1) are maps to slit domains satisfying certain boundary conditions and we use a least squares approach to find Laurent series which satisfy the boundary conditions. This method was used by the authors in [7,9] following, for instance, in [4,13,18].

Other possible factorizations were discussed in [3,9]. The Schwarz–Christoffel transformations for unbounded multiply connected domains can also be written in terms of finite products of Schottky–Klein prime functions [2]. The prime functions can also be computed using Laurent series [4]. We plan to compare the various approaches computationally and discuss other potential numerical and theoretical improvements in future work. In addition, it should be possible to develop similar methods for the bounded case [5]. However, the significant increase in efficiency, accuracy, and connectivity afforded by our current approach merits reporting at this time.

This paper is organized as follows. In Sect. 2, we introduce notation and basic useful information. In Sect. 3, we explore replacing the infinite product of reflections in (1) with finite products of slit maps; these slit maps are then computed using a least squares method. In Sect. 4, we briefly recall the numerical setup for the parameter problem and introduce an accuracy measurement. Finally, in Sect. 5, we present some numerical examples.

2 Preliminaries

We shall introduce notation, recall basic facts about reflections in circles, and state-related useful information. Complete discussions are given in [8,10], and in [9] with a sample reflection code. As already mentioned, $w = f(z)$ is a conformal map $f : \Omega \to \mathbb{P}$ from a circle domain to a polygonal domain of connectivity m, with c_j and r_j denoting the centers and radii, respectively, of the boundary circles C_j of Ω.

The *reflection* of a point z through a circle C with center c and radius r is given by

$$z^* = \rho_C(z) := c + \frac{r^2}{\overline{z} - \overline{c}},$$

i.e., z and z^* are symmetric points with respect to the circle C. If $z \in C$ then $z^* = z$, so that trivially $\rho_C(C) = C$. Given any two mutually exclusive circles C_τ, C_λ, the reflection of C_τ through C_λ is denoted $C_{\lambda\tau} = \rho_\lambda(C_\tau) := \rho_{C_\lambda}(C_\tau)$.

Lemma 1 [8, Prop. 1]

$$\rho_\lambda(\rho_\tau(z)) = \rho_{\lambda\tau}(\rho_\lambda(z)). \tag{2}$$

Proof Recall that Möbius transformations preserve reflections in circles and straight lines, so let C_λ be the real axis, where reflection is just complex conjugation. Then

$$\rho_\lambda(\rho_\tau(z)) = \overline{\rho_\tau(z)} = \rho_{\lambda\tau}(\overline{z}) = \rho_{\lambda\tau}(\rho_\lambda(z)).$$

□

Note that the order in which reflections are carried out is important, i.e., in general $\rho_\lambda(\rho_\tau(z)) \neq \rho_\tau(\rho_\lambda(z))$.

Definition 1 The set of multi-indices ν of length $|\nu| = n > 0$ is denoted

$$\sigma_n = \{\nu_1\nu_2\cdots\nu_n : 1 \le \nu_i \le m \text{ for } i=1,\ldots,n; \text{ and } \nu_i \ne \nu_{i+1} \text{ for } i=1,\ldots,n-1\},$$

with $\sigma_0 := \phi$. (If $\nu \in \sigma_0$, then we write for convenience $\nu j = j$). Also

$$\sigma_n(j) = \{\nu \in \sigma_n : \nu_n \ne j\},$$

denotes sequences in σ_n whose last factor never equals j.

An arbitrary reflected circle is denoted by C_ν with a multi-index ν labeling the sequence of reflections. Consider for example an unbounded circle domain with $m = 3$. For $|\nu| = 3$, three levels of reflection, the set of multi-indices would be

$$\sigma_3 = \{121, 123, 131, 132, 212, 213, 231, 232, 312, 313, 321, 323\}$$

with

$$\sigma_3(1) = \{123, 132, 212, 213, 232, 312, 313, 323\}.$$

The reflections of circles C_2 and C_3 through circle C_1 are $C_{12} = \rho_1(C_2)$ and $C_{13} = \rho_1(C_3)$, respectively. The reflection process is continued with, for instance, the circle C_1 reflected through C_{12} for $C_{121} = \rho_{12}(C_1) = \rho_{12}(\rho_1(C_1)) = \rho_1(\rho_2(C_1))$ by an application of (2), and C_{13} reflected through C_{12} for $C_{123} = \rho_{12}(C_{13}) = \rho_{12}(\rho_1(C_3)) = \rho_1(\rho_2(C_3))$, etc. See Fig. 1. Some care is required to reconstruct the original sequence of reflections from the index ν, as illustrated by C_{123}. However note that, more generally, $C_\nu = C_{\nu_1\nu_2\cdots\nu_n}$ is in the interior of C_{ν_1} and arises from a sequence of reflections of C_{ν_n}.

Use of the radii and centers of the reflected circles, as well as the reflections of the centers of the boundary circles of Ω, will be required. The radius of a reflected circle $C_{\nu j}$ will be denoted $r_{\nu j}$, and let $c_{\nu j}$ be the center of such a circle. To make a distinction between centers of reflected circles and reflections of the centers of the $C_j \in \partial\Omega$, set $s_j = c_j$ so that $s_{\nu j}$ represents the latter. It is clear that $s_{\nu j} \ne c_{\nu j}$ for $\nu \in \sigma_n(j), n > 0$.

Repeated use of (2) shows that reflection through any circle C_ν can be factored into a sequence of reflections solely through the $C_j \in \partial\Omega$, which greatly simplifies the numerical computation of these reflections. This factoring is expressed in the following form of [8, Lemma 1].

Lemma 2 *For* $\nu = \nu_1\nu_2\cdots\nu_n \in \sigma_n(j)$,

$$C_{\nu j} = \rho_{\nu_1}(\rho_{\nu_2}(\cdots(\rho_{\nu_n}(C_j))\cdots)), \text{ and}$$
$$s_{\nu j} = \rho_{\nu_1}(\rho_{\nu_2}(\cdots(\rho_{\nu_n}(s_j))\cdots)).$$

The proof of [8, Lemma 1] uses (2) and an induction argument, which will not be given here, to show that, *e.g.*, $C_{\nu j} = \rho_{\nu_1}(C_{\nu_2\cdots\nu_n j})$. Repeated application of this to ν_2 through ν_n gives the Lemma.

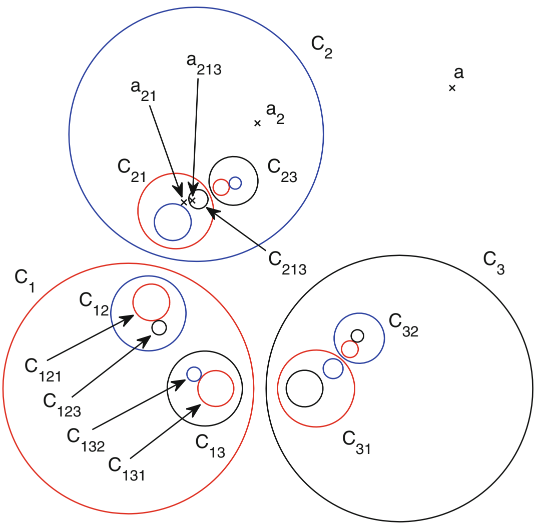

Fig. 1 An example of reflected circles to a level of $|\nu| = 3$. The point $a_{213} = \rho_{213}(\rho_{21}(\rho_2(a)))$ is also shown

Similarly, for any $a \in \Omega$, let $a_\nu := \rho_{\nu_1}(\rho_{\nu_2}(\cdots(\rho_{\nu_n}(a))\cdots))$. Then given, for example, a point a_{213}, one may reconstruct the original sequence of reflections, by the use of (2),

$$a_{213} = \rho_2(\rho_1(\rho_3(a))) = \rho_2(\rho_{13}(\rho_1(a)))$$
$$= \rho_{213}(\rho_2(\rho_1(a))) = \rho_{213}(\rho_{21}(\rho_2(a))).$$

This is a reflected through C_2, which is then reflected through C_{21}, and the result is then reflected through $C_{213} = \rho_{21}(C_{23})$. See Fig. 1.

Based on Lemma 2, a routine was developed in MATLAB which performs the reflections of centers of boundary circles and points on these circles to some specified level $|\nu| = N$. Only reflections across the original circles are computed. For instance, $a_{123} = \rho_{123}(a_{12})$ is computed as $a_{123} = \rho_1(\rho_2(\rho_3(a)))$. The code stores an expanding array of integers, $j \in \{1, \ldots, m\}$, for each reflection such that ρ_j is the most recent reflection. For the next level of reflections, ρ_j is then skipped, since $\rho_j(\rho_j(a)) = a$. It should be noted that for a given $|\nu| = n > 0$, the set σ_n has $|\sigma_n| = m(m-1)^{n-1}$ elements. This exponential increase in size is a principle difficulty in computing maps in terms of these reflections.

We need the following definition and lemma for the statement of our convergence results. The *separation parameter* of the region is

$$\Delta := \max_{i,j;i\neq j} \frac{r_i + r_j}{|c_i - c_j|} < 1, \quad 1 \le i, j \le m \tag{3}$$

for the assembly of m mutually exterior circles that form the boundary of Ω, cf. [14, p. 501]. Let $\widetilde{C}_j$ denote the circle with center c_j and radius r_j/Δ. Then geometrically, $1/\Delta$ is the smallest magnification of the m radii such that at least two $\widetilde{C}_j$'s just

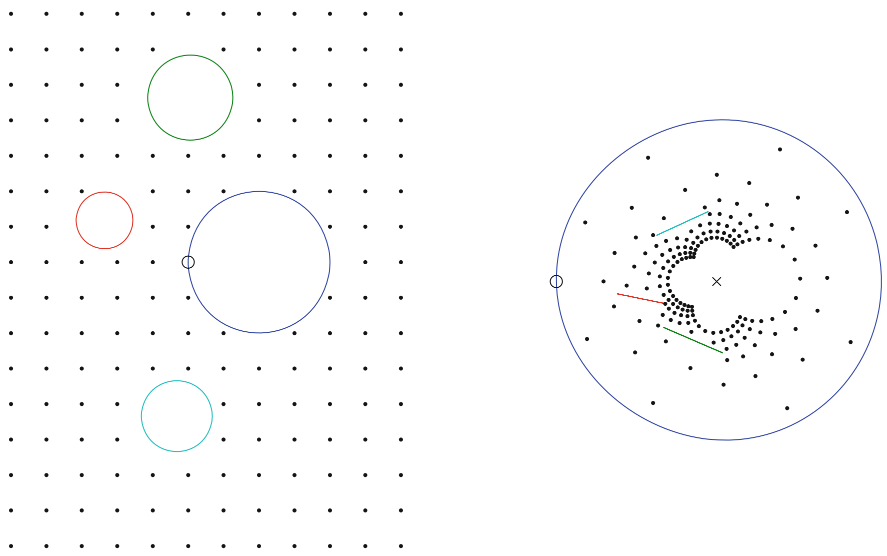

Fig. 2 Map $w = f_{z_{k,j}}(z)$ from the exterior of four disks to the interior of a convex curve through 0 with three radial slits removed. The point $z_{k,j}$ in the z-plane (marked by 'O') is mapped to the origin 0 in the w-plane and $f_{z_{k,j}}(\infty) = 1$ marked by an 'X'. The other circles are mapped to the radial slits. This map was computed with the reflection algorithm with $N = 3$ levels of reflection

touch. The following inequality from [14, p. 505] then gives us an estimate of the rate of decrease of the areas of the reflected circles.

Lemma 3

$$\sum_{\nu \in \sigma_{n+1}} r_\nu^2 \leq \Delta^{4n} \sum_{j=1}^{m} r_j^2. \tag{4}$$

3 Finite Product Representation for the Derivative of the Map

We give a new version of (1) where the integrand is in terms of finite products of maps, $f_{z_{k,j}}(z)$ from the exterior circle domains to the interior of a curve through and star-like with respect to the origin with radial slits removed; see Figs. 2 and 3. The final multiply connected Schwarz–Christoffel (MCSC) formula will be a minor modification of the original formula (1), where the inner infinite products are replaced by these radial slit maps. The formula is

$$f(z) = \int^{z} \prod_{j=1}^{m} \prod_{k=1}^{K_j} \left[f_{z_{k,j}}(\zeta) \right]^{\beta_{k,j}} \mathrm{d}\zeta. \tag{5}$$

Here $f_{z_{k,j}}(z)$ is the map just described with $f_{z_{k,j}}(z_{k,j}) = 0$ and $f_{z_{k,j}}(\infty) = 1$.

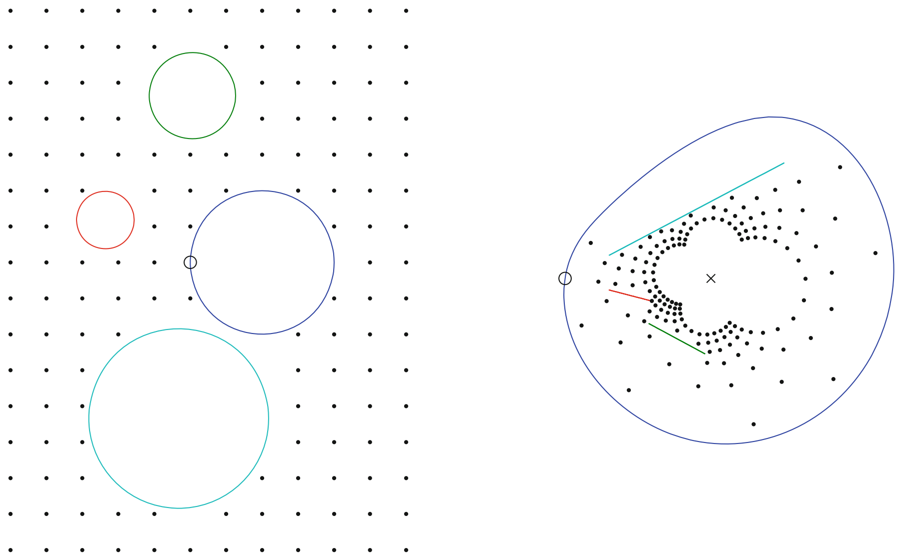

Fig. 3 Another example with $N = 5$ levels of reflection. Note the star-likeness with respect to 0 of the image region

If the domain satisfies the separation condition $\Delta < (m-1)^{-1/4}$ from [6,8], then we can represent $f_{z_{k,j}}(z)$ explicitly as an infinite product,

$$f_{z_{k,j}}(z) := \prod_{\substack{n=0 \\ \nu \in \sigma_n(j)}}^{\infty} \left(\frac{z - z_{k,\nu j}}{z - s_{\nu j}} \right) \tag{6}$$

where $z_{k,\nu j}$ and $s_{\nu j}$ are reflections of the prevertex $z_{k,j}$ and the center $s_j = c_j$, respectively, on the jth circle. For instance, for the $k = 2$ prevertex on circle $j = 1$ with $m = 3$

$$f_{z_{2,1}}(z) = \frac{(z - z_{2,1})(z - z_{2,21})(z - z_{2,31})(z - z_{2,121}) \cdots}{(z - s_1)(z - s_{21})(z - s_{31})(z - s_{121}) \cdots}. \tag{7}$$

Note that these maps *are not* the maps to canonical radial slit domains given in [6]. For instance, the poles at the other centers s_p, $p \neq j$, and their reflections are missing from the infinite product. Only s_j for one fixed j is reflected.

Remark 1 In [9], we expressed the formula as

$$f'(z) = A f_a(z) \prod_{j=1}^{m} \prod_{k=1}^{K_j} \left[f_{k,j}(z) \right]^{\beta_{k,j}} \tag{8}$$

where, for arbitrarily chosen $a_j \in C_j$, $a_j \neq z_{k,j}$,

$$f_{k,j}(z) = \prod_{\substack{n=0 \\ \nu\in\sigma_n(j)}}^{\infty} \left(\frac{z - z_{k,\nu j}}{z - a_{\nu j}}\right) \tag{9}$$

are maps to radially slit half-planes with $f_{k,j}(z_{k,\nu j}) = 0$ and $f_{k,j}(a_{\nu j}) = \infty$, and

$$f_a(z) := \left(\prod_{j=1}^{m} f_{a_j}(z)\right)^2 \quad \text{with} \quad f_{a_j}(z) := \prod_{\substack{n=0 \\ \nu\in\sigma_n(j)}}^{\infty} \left(\frac{z - a_{\nu j}}{z - s_{\nu j}}\right). \tag{10}$$

Note that the $f_{a_j}(z)$ are exactly the maps of the form $f_{z_{k,j}}(z)$ with the arbitrarily selected a_j's replacing the prevertices, $z_{k,j}$. While this factorization in terms of maps to radially slit half planes has some theoretical and geometric appeal (see also [3]), we will not discuss its numerical implementation here.

Finally, we note that forms above fit into the framework of [12] where the derivative of the mapping function, $f'(z)$, is expressed as a product,

$$f'(z) = A \prod_k f_k(z), \tag{11}$$

of factors $f_k(z)$ that guarantee that f' has piecewise constant argument for the given geometry. For instance, for the case of simply connected maps from the disk, $f_k(z) := (z - z_j)^{\beta_k}$, $-\beta_k\pi$ is the turning angle at prevertex z_k, $\beta_k = \alpha_k - 1$, and $\sum_k \beta_k = -2$. In this case, the mapping function is

$$f(z) = A \int^{z} \prod_k (\zeta - z_k)^{\beta_k} \mathrm{d}\zeta + B, \tag{12}$$

where a normalization condition, such as fixing an interior point and one boundary point, gives a unique map. There are several variations in which other domains are used, e.g., a rectangle or an infinite strip, [12, Chap. 4].

3.1 Properties of the Unbounded Map Factors from an Infinite Product Representation

Let a_j be a point on one of the boundary circles C_j. In terms of reflections we may write

$$f_{a_j}(z) = \prod_{\substack{n=0 \\ \nu\in\sigma_n(j)}}^{\infty} \left(\frac{z - a_{\nu j}}{z - s_{\nu j}}\right). \tag{13}$$

If $a_j = z_{k,j}$, then f_{a_j} is one of the factors of the unbounded MCSC map.

We can define a *singularity function* $S_{a_j}(z)$ for f_{a_j} as

$$S_{a_j}(z) := \frac{f'_{a_j}(z)}{f_{a_j}(z)} = \frac{d}{dz} \log f_{a_j}(z) = \sum_{\substack{n=0 \\ \nu\in\sigma_n(j)}}^{\infty} \left(\frac{1}{z - a_{\nu j}} - \frac{1}{z - s_{\nu j}} \right). \tag{14}$$

The proof of convergence of S_{a_j} closely follows [7, Theorem 3.3] with the sums over $j = 1, \ldots, m$ eliminated. We will show that the sums truncated to N levels of reflection,

$$S_{a_j,N}(z) = \sum_{\substack{n=0 \\ \nu\in\sigma_n(j)}}^{N} \left(\frac{1}{z - a_{\nu j}} - \frac{1}{z - s_{\nu j}} \right), \tag{15}$$

converge uniformly to $S_{a_j}(z)$ for $z \in \overline{\Omega}$ as $N \to \infty$, provided the circles satisfy the separation condition, and so $f_{a_j}(z) = \exp(\int S_{a_j}(z)\,dz)$. In the special case when $m = 2$ there is no restrictive separation hypothesis since then $\Delta < (m-1)^{-1/4} = 1$ is equivalent to the fact that the two boundary components are disjoint.

We now prove the convergence of $S_{a_j,N}(z)$ to $S_{a_j}(z)$ for sufficiently well-separated circles.

Theorem 4 *For connectivity $m \geq 2$, $S_{a_j,N}(z)$ converges to $S_{a_j}(z)$ uniformly on $\overline{\Omega}$ such that*

$$|S_{a_j}(z) - S_{a_j,N}(z)| = O\left((\Delta^2 \sqrt{m-1})^N \right) \tag{16}$$

for regions satisfying the separation condition

$$\Delta < \frac{1}{(m-1)^{1/4}}. \tag{17}$$

Proof For $n = 0, 1, 2, \ldots,$ we write

$$A_{a_j,n}(z) = \sum_{\nu\in\sigma_n(j)} \left(\frac{1}{z - a_{\nu j}} - \frac{1}{z - s_{\nu j}} \right) = \sum_{\nu\in\sigma_n(j)} \frac{a_{\nu j} - s_{\nu j}}{(z - a_{\nu j})(z - s_{\nu j})} \tag{18}$$

and hence,

$$S_{a_j,N}(z) = \sum_{n=0}^{N} A_{a_j,n}(z). \tag{19}$$

Let

$$\delta = \delta_\Omega = \inf_{z\in\Omega} \{|z - a_\nu|, |z - s_\nu| : \nu \in \sigma_n, n = 1, 2, 3, \ldots\}. \tag{20}$$

Clearly $\delta > 0$ since points a_ν and s_ν lie inside the boundary circles of Ω. Note that the number of terms in the $A_{a_j,n}(z)$ sum is $O((m-1)^n)$. This exponential increase in the number of terms is the principal difficulty in establishing convergence. Recall that $r_{\nu j}$ is the radius of circle $C_{\nu j}$. We bound $A_{a_j,n}(z)$ for $z \in \overline{\Omega}$ by using $|a_{\nu j} - s_{\nu j}| < 2r_{\nu j}$, and the Cauchy–Schwarz inequality, as follows:

$$\begin{aligned}
|A_{a_j,n}(z)| &\le \sum_{\nu\in\sigma_n(j)} \frac{|a_{\nu j} - s_{\nu j}|}{|z - a_{\nu j}||z - s_{\nu j}|} \\
&\le \frac{2}{\delta^2} \sum_{\nu\in\sigma_n(n)} r_{\nu j} \\
&\le \frac{2}{\delta^2} \left(\sum_{\nu\in\sigma_n(j)} r_{\nu j}^2 \right)^{1/2} \left(\sum_{\nu\in\sigma_n(j)} 1 \right)^{1/2} \\
&= \frac{2}{\delta^2} \left(\sum_{\nu\in\sigma_n(j)} r_{\nu j}^2 \right)^{1/2} (m-1)^{n/2} \\
&< \frac{2}{\delta^2} \Delta^{2n} \left(\sum_{j=1}^{m} r_j^2 \right)^{1/2} (m-1)^{n/2} \\
&\le C\Delta^{2n}(m-1)^{n/2}
\end{aligned} \tag{21}$$

by Lemma 3 where $\delta = \delta_\Omega$. Therefore, by the Weierstrass M-test, the series converges uniformly to $S_{a_j}(z) = \lim_{N\to\infty} S_{a_j,N}(z)$, if $\Delta^2\sqrt{m-1} < 1$. □

Our boundary conditions for f_{a_j} are given by the following lemma.

Lemma 5 *The function f_{a_j} satisfies*

$$\arg f_{a_j}(z) = \text{const.} \quad \textit{for} \quad z \in C_p,\ p \ne j,$$

i.e., f_{a_j} maps the circles C_p, $p \ne j$ to radial slits with respect to the origin, if and only if

$$\mathrm{Re}\left\{ (z - c_p)\frac{f'_{a_j}(z)}{f_{a_j}(z)} \right\} = 0 \quad \textit{for} \quad z \in C_p.$$

Proof For $z \in C_p$, we have $z = c_p + r_p e^{i\theta}$ and since $f_{a_j}(z)$ maps to radial slits, we have arg $f(z)$ =const. Therefore,

$$0 = \frac{\partial}{\partial\theta} \arg f(z) = \frac{\partial}{\partial\theta} \operatorname{Im}\left\{\log f(c_p + r_p e^{i\theta})\right\}$$
$$= \operatorname{Im}\left\{ i r_p e^{i\theta} \frac{f'}{f} \right\} = \operatorname{Re}\left\{ r_p e^{i\theta} \frac{f'}{f}(c_p + r_p e^{i\theta}) \right\}.$$

□

The proof that $f_{a_j}(z)$ defined by the (convergent) infinite product formula satisfies the boundary conditions in Lemma 5 is nearly identical to [7, Theorem 3.4]. Again, we will use the formula

$$\operatorname{Re}\left\{ \frac{w}{w-1} + \frac{w^*}{w^*-1} \right\} = 1 \tag{22}$$

where w and $w^* = 1/\overline{w}$ are symmetric points with respect to the unit circle. Then the following theorem gives the desired result. (Recall that $s_p = c_p$).

Theorem 6 *If* $\Delta < (m-1)^{-1/4}$ *then for* $z \in C_p$, $p \neq j$,

$$\operatorname{Re}\left\{(z - s_p) S_{a_j,N}(z)\right\} = O((\Delta^2 \sqrt{m-1})^N)$$

and

$$\operatorname{Re}\left\{(z - s_p) S_{a_j}(z)\right\} = 0$$

Proof The idea of the proof is, for $z \in C_p$, to use properties of the reflections in Lemma 2 to group terms in $S_{a_j,N}(z)$ related by reflection ρ_p through C_p with $z \in C_p$ as follows:

$$S_{a_j,N}(z) = \left(\frac{1}{z - a_j} + \frac{1}{z - a_{pj}}\right) - \left(\frac{1}{z - s_j} + \frac{1}{z - s_{pj}}\right) + \cdots$$
$$+ \left(\frac{1}{z - a_{\nu j}} + \frac{1}{z - a_{p\nu j}}\right) - \left(\frac{1}{z - s_{\nu j}} + \frac{1}{z - s_{p\nu j}}\right) + \cdots. \tag{23}$$

Then, multiplying by $z - s_p$, we have in more detail,

$$(z - s_p) S_{a_j,N}(z) = \frac{(z - s_p)/(a_j - s_p)}{(z - s_p)/(a_j - s_p) - 1} + \frac{(z - s_p)/(a_{pj} - s_p)}{(z - s_p)/(a_{pj} - s_p) - 1}$$
$$- \frac{(z - s_p)/(s_j - s_p)}{(z - s_p)/(s_j - s_p) - 1} + \frac{(z - s_p)/(s_{pj} - s_p)}{(z - s_p)/(s_{pj} - s_p) - 1}$$

$$+\sum_{n=1}^{N-1}\sum_{\substack{\nu\in\sigma_n(j),\\ \nu_1\neq p}}\left(\frac{(z-s_p)/(a_{\nu j}-s_p)}{(z-s_p)/(a_{\nu j}-s_p)-1}+\frac{(z-s_p)/(a_{p\nu j}-s_p)}{(z-s_p)/(a_{p\nu j}-s_p)-1}\right) \quad (24)$$

$$-\sum_{n=1}^{N-1}\sum_{\substack{\nu\in\sigma_n(j)\\ \nu_1\neq p}}\left(\frac{(z-s_p)/(s_{\nu j}-s_p)}{(z-s_p)/(s_{\nu j}-s_p)-1}+\frac{(z-s_p)/(s_{p\nu j}-s_p)}{(z-s_p)/(s_{p\nu j}-s_p)-1}\right)$$

$$+(z-s_p)\sum_{\substack{\nu\in\sigma_N(j),\\ \nu_1\neq p}}\left(\frac{a_{\nu j}-s_{\nu j}}{(z-a_{\nu j})(z-s_{\nu j})}\right).$$

We take the real part of the above expression and, using, for instance, $w = (z-s_p)/(a_{\nu j}-s_p)$ and noting that $w^* = (z-s_p)/(a_{p\nu j}-s_p)$, (22) gives

$$\mathrm{Re}\left\{\frac{(z-s_p)/(a_{\nu j}-s_p)}{(z-s_p)/(a_{\nu j}-s_p)-1}+\frac{(z-s_p)/(a_{p\nu j}-s_p)}{(z-s_p)/(a_{p\nu j}-s_p)-1}\right\}$$
$$= \mathrm{Re}\left\{\frac{w}{w-1}+\frac{w^*}{w^*-1}\right\} = 1. \quad (25)$$

Taking the real part of (24), we see that the first four lines sum to 0. The final terms, all lying inside circles C_j, $j \neq p$, approximate the truncation error and are estimated by Lemma 3. This gives our final result

$$\mathrm{Re}\left\{(z-s_p)S_N(z)\right\} = O\left(\left(\Delta^2\sqrt{m-1}\right)^N\right). \quad (26)$$

□

Next, we prove the boundary condition for $z = s_j + r_j e^{i\theta} \in C_j$, that $\partial \arg f_{a_j}(z)/\partial\theta = -1/2$.

Theorem 7 *If* $\Delta < (m-1)^{-1/4}$ *then for* $z \in C_j$,

$$\mathrm{Re}\left\{(z-s_j)S_{a_j,N}(z)\right\} = -1/2 + O((\Delta^2\sqrt{m-1})^N)$$

and

$$\mathrm{Re}\left\{(z-s_j)S_{a_j}(z)\right\} = -1/2.$$

Proof Multiplying $S_{a_j,N}(z)$ by $(z-s_j)$ and grouping terms by reflection across circle C_j gives

$$(z-s_j)S_{a_j,N}(z) = (z-s_j)\left[\frac{1}{z-a_j}-\frac{1}{z-s_j}\right]+\cdots$$
$$+\left(\frac{z-s_j}{z-a_{\nu j}}+\frac{z-s_j}{z-a_{j\nu j}}\right)-\left(\frac{z-s_j}{z-s_{\nu j}}+\frac{z-s_j}{z-s_{j\nu j}}\right)+\cdots$$

$$
\begin{aligned}
&= -1 + \frac{z - s_j}{z - a_j} \\
&\quad + \sum_{n=1}^{N-1} \sum_{\substack{\nu \in \sigma_n(j) \\ \nu_1 \neq j}} \left[\frac{(z-s_j)/(a_{\nu j} - s_j)}{(z-s_j)/(a_{\nu j}-s_j) - 1} + \frac{(z-s_j)/(a_{j\nu j} - s_j)}{(z-s_j)/(a_{j\nu j}) - 1} \right] \\
&\quad - \sum_{n=1}^{N-1} \sum_{\substack{\nu \in \sigma_n(j) \\ \nu_1 \neq j}} \left[\frac{(z-s_j)/(s_{\nu j} - s_j)}{(z-s_j)/(s_{\nu j}-s_j) - 1} + \frac{(z-s_j)/(s_{j\nu j} - s_j)}{(z-s_j)/(s_{j\nu j}) - 1} \right] \\
&\quad + (z - s_j) \sum_{\substack{\nu \in \sigma_N(j) \\ \nu_1 \neq j}} \frac{a_{\nu j} - s_{\nu j}}{(z - a_{\nu j})(z - s_{\nu j})}.
\end{aligned}
$$

Then using $z = s_j + r_j e^{i\theta}$ and $a_j = s_j + r_j e^{i\theta_j}$, noticing the real part of the first sum cancels with the real part of the second sum as in the previous proof, and bounding the last sum of the equation as before, we get

$$
\begin{aligned}
\operatorname{Re}\left\{(z - s_j) S_{a_j,N}(z)\right\} &= -1 + \operatorname{Re}\left\{\frac{e^{i\theta}}{e^{i\theta} - e^{i\theta_j}}\right\} + O\left(\left(\Delta^2 \sqrt{m-1}\right)^N\right) \\
&= -1 + \operatorname{Re}\left\{\frac{e^{i(\theta-\theta_j)/2}}{e^{i(\theta-\theta_j)/2} - e^{-i(\theta-\theta_j)/2}}\right\} + O\left(\left(\Delta^2 \sqrt{m-1}\right)^N\right) \\
&= -1 + \operatorname{Re}\left\{\frac{1}{2} - \frac{i}{2} \cot \frac{\theta - \theta_j}{2}\right\} + O\left(\left(\Delta^2 \sqrt{m-1}\right)^N\right) \\
&= -\frac{1}{2} + O\left(\left(\Delta^2 \sqrt{m-1}\right)^N\right).
\end{aligned}
$$

□

3.2 Boundary Value Problem for the Finite Product Representation

The results in the previous section show that the infinite product representations for the $f_{a_j}(z)$'s are analytic functions in the circle domain satisfying certain boundary conditions and a condition at infinity. We conjecture that these conditions, in general, define a conformal map $f_{a_j}(z)$ to star-like domains with radial slits for arbitrary circle domains which need not satisfy the separation condition, $\Delta < (m-1)^{-1/4}$, as illustrated in our computations.

Conjecture 1 *If* $f_{a_j}(a_j) = 0$, $f_{a_j}(\infty) = 1$, *with the boundary conditions*

1. $\arg f_{a_j}(z) = \text{const.}$ *for* $z \in C_p$, $p \neq j$ *and*
2. $\partial \arg f_{a_j}(z)/\partial\theta = -1/2$ *for* $z = s_j + r_j e^{i\theta} \in C_j$,

then $f_{a_j}(z)$ *is a uniquely determined conformal map from the circle domain to the interior of a domain bounded by a curve* $\Gamma_j = f_{a_j}(C_j)$ *through the origin and* *star-like with respect to the origin and by interior radial slits* $\Gamma_p = f_{a_j}(C_p)$, $p \neq j$.

In the next section, these maps will be computed using Laurent series approximations. Note that the singularity functions $S_{a_j}(z) = f'_{a_j}(z)/f_{a_j}(z)$ are solutions to a Riemann–Hilbert problem for the multiply connected circle domains. Recent results on the theory of such problems should be applicable, but we will not discuss this here; see, e.g. [16].

Using the maps $f_{z_{k,j}}(z)$, a general formula for the multiply connected Schwarz–Christoffel map involving only finite products and not requiring the separation condition, can be written as

$$f(z) = A \int^{z} \prod_{j=1}^{m} \prod_{k=1}^{K_j} \left[f_{z_{k,j}}(\zeta) \right]^{\beta_{k,j}} \mathrm{d}\zeta + B.$$

Note that

$$S(z) := f''(z)/f'(z) = \sum_{j=1}^{m} \sum_{k=1}^{K_j} \beta_{k,j} S_{z_{k,j}}(z). \tag{27}$$

Then since

$$\left(-\frac{1}{2}\right) \sum_{k=1}^{K_j} \beta_{k,j} = -1, \tag{28}$$

$S(z)$ will satisfy the boundary conditions from [8],

$$\mathrm{Re}\left\{(z - c_j) S(z)\right\}_{z \in C_j} = -1. \tag{29}$$

Example 1 The Joukowski map $f(z) = z + 1/z$ provides a simple example of the form of our SC formula for the simply connected case. In this case, the prevertices are $z_1 = 1$ and $z_2 = -1$, $\beta_1 = \beta_2 = 1$, and we may write

$$f'(z) = 1 - \frac{1}{z^2} = \frac{z^2 - 1}{z^2} = \frac{z-1}{z}\frac{z+1}{z} = f_1(z) f_{-1}(z). \tag{30}$$

The boundary conditions on $z = e^{i\theta}$ are

$$\mathrm{Re}\left\{ z \frac{f'_{\pm 1}(z)}{f_{\pm 1}(z)} \right\} = \mathrm{Re}\left\{ \pm \frac{1}{z - (\pm 1)} \right\} = -\frac{1}{2}. \tag{31}$$

A conformal map of the exterior of the unit disk to the exterior of a bounded polygon provides a simple example.

3.3 Computation of the Unbounded Map Factors

Following the ideas presented in [4,7,9,13,18], we seek a series representation of f_{a_j} since, as will be shown below, it is possible to state the boundary conditions linearly in terms of the coefficients of the series. We begin by writing the function in the form

$$f_{a_j}(z) = \frac{z - a_j}{z - s_j} e^{g(z)}, \tag{32}$$

where g is analytic in the domain and $g(z) \to 0$ as $z \to \infty$. Then $f_{a_j}(a_j) = 0$ and $f_{a_j}(\infty) = 1$, as required. The function g is given as the sum of the Laurent series expansions on the exterior of each boundary circle,

$$g(z) = \sum_{p=1}^{m} \sum_{\ell=1}^{\infty} \frac{d_{\ell,p} r_p^{\ell}}{(z - s_p)^{\ell}}. \tag{33}$$

Since $\operatorname{Im}\left\{\log f_{a_j}\right\} = \arg f_{a_j}$, the boundary conditions given in Lemma 5 and Theorem 7 above are now

$$\operatorname{Im}\left\{\log f_{a_j}\right\} \equiv \text{const.}, \quad \text{for all } z \in C_p, \quad p \neq j \tag{34}$$

and

$$\frac{\partial}{\partial\theta} \operatorname{Im}\left\{\log f_{a_j}\right\} = -\frac{1}{2}, \quad \text{for all } z \in C_j. \tag{35}$$

Note for $z = s_j + r_j e^{i\theta}$,

$$\frac{\partial}{\partial\theta} \operatorname{Im}\left\{\log f_{a_j}(z)\right\} = \operatorname{Im}\left\{ i r_j e^{i\theta} \frac{f'_{a_j}(z)}{f_{a_j}(z)} \right\} = \operatorname{Re}\left\{ (z - s_j) \frac{f'_{a_j}(z)}{f_{a_j}(z)} \right\} \tag{36}$$

where

$$\frac{f'_{a_j}(z)}{f_{a_j}(z)} = \frac{d}{dz} \log f_{a_j}(z) = \frac{1}{z - a_j} - \frac{1}{z - s_j} + g'(z) \tag{37}$$

which gives

$$\operatorname{Re}\left\{ (z - s_j) \frac{f'_{a_j}(z)}{f_{a_j}(z)} \right\} = \operatorname{Re}\left\{ \frac{z - s_j}{z - a_j} - 1 + (z - s_j) g'(z) \right\} = -\frac{1}{2}. \tag{38}$$

By the calculation used in the proof of Theorem 7 we know that

$$\operatorname{Re}\left\{ \frac{z - s_j}{z - a_j} \right\} = \frac{1}{2}. \tag{39}$$

The boundary conditions may thus be restated in terms of g by

$$\text{Im}\{g(z)\} = \text{const.} - \arg\frac{z-a_j}{z-s_j}, \quad \text{for all } z \in C_p, \quad p \neq j; \tag{40}$$

$$\text{Re}\left\{(z-s_j)g'(z)\right\} = 0, \quad \text{for all } z \in C_j. \tag{41}$$

The coefficients $d_{\ell,p}$ of g are found by solving a linear system of equations based on these conditions.

For computation we discretize by truncating the series in ℓ for g after N terms, and choose M points z on each boundary circle. Let $x = [d_{\ell,p}]$ be the $(mN \times 1)$ column vector of coefficients. Define for $p = 1, \ldots, m$ the matrices

$$F_p = \left[r_p^\ell (z-s_p)^{-\ell}\right]_{M\times mN} \quad \text{for} \quad z \in C_p,\ p \neq j. \tag{42}$$

Based on

$$g'(z) \approx \sum_{p=1}^{m}\sum_{\ell=1}^{N} \frac{-\ell d_{\ell,p} r_p^\ell}{(z-s_p)^{\ell+1}} \tag{43}$$

define

$$G = \left[-\ell(z-s_j) r_p^\ell (z-s_p)^{-\ell-1)}\right]_{M\times mN} \quad \text{for} \quad z \in C_j. \tag{44}$$

With $F_p = F_{R_p} + iF_{I_p}$, $G = G_R + iG_I$, and $x = x_R + ix_I$ a calculation shows

$$\text{Im}\{g(z)\} \approx F_{I_p} x_R + F_{R_p} x_I \quad \text{on any} \quad C_p,\ p \neq j \tag{45}$$

and

$$\text{Re}\left\{(z-s_j)g'(z)\right\} \approx G_R x_R - G_I x_I \quad \text{on} \quad C_j. \tag{46}$$

The values of $\text{Im}(f_{a_j})$ may not be known in advance, but the difference of $\text{Im}(f_{a_j})$ for any pair of points on a circle C_p, $p \neq j$, is zero. Then define

$$P = \begin{bmatrix} -1 & 1 & & & \\ & -1 & 1 & & \\ & & \ddots & \ddots & \\ & & & -1 & 1 \end{bmatrix}_{M-1\times M} \tag{47}$$

so that for $z \in C_p$ we have

$$P\left[F_{I_p}\ F_{R_p}\right]\begin{bmatrix} x_R \\ x_I \end{bmatrix} = -P\left[\arg\frac{z-a_j}{z-s_j}\right]_{M\times 1} \tag{48}$$

by the boundary condition (40). By the boundary condition (41) it is also the case that

$$\left[\, G_R \; -G_I \,\right] \begin{bmatrix} x_R \\ x_I \end{bmatrix} = \left[\, 0 \,\right]. \tag{49}$$

For the sake of exposition suppose $j \notin \{1, m\}$. Define the block matrices

$$B_1 = \begin{bmatrix} F_{I_1} \\ \vdots \\ F_{I_{j-1}} \\ G_R \\ F_{I_{j+1}} \\ \vdots \\ F_{I_m} \end{bmatrix}_{mM \times mN} \quad \text{and} \quad B_2 = \begin{bmatrix} F_{R_1} \\ \vdots \\ F_{R_{j-1}} \\ -G_I \\ F_{R_{j+1}} \\ \vdots \\ F_{R_m} \end{bmatrix}_{mM \times mN} \tag{50}$$

and the difference matrix

$$E = \begin{bmatrix} P & & & & \\ & \ddots & & & \\ & & I & & \\ & & & \ddots & \\ & & & & P \end{bmatrix}_{m(M-1)+1 \times mM} \tag{51}$$

where the identity matrix occupies the jth block-row. A least squares solution to the system

$$E \left[\, B_1 \;\; B_2 \,\right] \begin{bmatrix} x_R \\ x_I \end{bmatrix} = -E \begin{bmatrix} \arg \frac{z-a_j}{z-s_j} \\ \vdots \\ 0 \\ \vdots \\ \arg \frac{z-a_j}{z-s_j} \end{bmatrix}_{mM \times 1} \tag{52}$$

using the MATLAB backslash operator gives the coefficients of g.

To choose the number of collocation points M, consider that for the system given by Eq. (52) to be square a calculation shows that M must satisfy

$$M = \frac{2mN + m - 1}{m}.$$

The ceiling function could be employed to allow for any truncation level N without regard to m, which would make the system overdetermined in the case M is not an integer. For consistency we just require that the system always be overdetermined by the inequality

$$M > \frac{2mN + m - 1}{m},$$

where

$$M = 2N + 1 = \frac{2mN + m}{m}$$

satisfies this condition.

4 Solution of the Parameter Problem

We will briefly recall some details of the numerical computation of Schwarz–Christoffel maps for unbounded multiply connected domains reported in [10]. Several examples of both bounded and unbounded domains are computed in [9, 10] using the reflection method.

In order to compute of the MCSC maps for given polygonal boundaries, we must solve the so-called *parameter problem* of finding the prevertices and the centers and radii of the circles. We do this by solving a non-linear set of equations, described below, that guarantee that the side lengths of the polygons and their locations are correct. Our method proves to be extremely robust and rarely fails to converge. A more complete discussion of the computational aspects and behavior of this setup is given in [10].

We now summarize some details for the unbounded maps from [10]. The prevertices on C_j are parametrized by $\theta_{k,j}$, where $z_{k,j} = c_j + r_j e^{i\theta_{k,j}}$ for $k = 1, \ldots, K_j$, and constrained to lie in order,

$$\theta_{1,j} < \theta_{2,j} < \cdots < \theta_{K_j,j}. \tag{53}$$

The unknown c_j's, r_j's, and $\theta_{k,j}$'s amount to a total of $K_1 + K_2 + \cdots + K_m + 3m$ real parameters. We approximate $f'(z)$ by $p(z)$ using Laurent series as described above. In the unbounded case, the map can be normalized as

$$f(z) = Az + B + O(1/z), \qquad z \to \infty,$$

by fixing one boundary point, $f(1) = w_{1,1}$ and C_1 as the unit circle. Letting

$$A = \frac{w_{2,1} - w_{1,1}}{\int_{z_{1,1}}^{z_{2,1}} p(z)\mathrm{d}z},$$

we have

$$f(z) = A \int_{z_{1,1}}^{z} p(\zeta)\, \mathrm{d}\zeta + B,$$

Fig. 4 Geometry used for Fig. 5

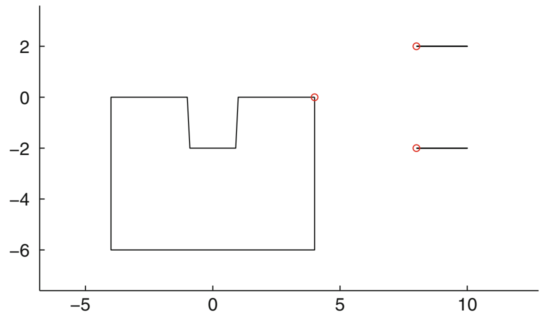

with $f(z_{1,1}) = B = w_{1,1}$. We require that $c_1 = 0$ and $r_1 = 1$, and fixing $f(1) = w_{1,1}$ is equivalent to setting $\theta_{1,1} = 0$. This amounts to fixing four of the real parameters, so that we have

$$K_1 + \cdots + K_m + 3m - 4$$

unknowns parameters to determine.

The remaining parameters are determined from the geometry of the polygonal domain. First, we have the *side-length conditions*,

$$|f(z_{k+1,j}) - f(z_{k,j})| = |w_{k+1,j} - w_{k,j}|,$$

for $j = 1, \ldots, m$ and $k = 1, \ldots, K_j$, where here and below

$$f(z_{k+1,j}) - f(z_{k,j}) = A \int_{z_{k,j}}^{z_{k+1,j}} p(\zeta)\, \mathrm{d}\zeta$$

is calculated by numerical integration. Compound Gauss–Jacobi integration as described in [12] (which includes the use of the "one-half rule"[1]) is used to handle the singularities in the Schwarz–Christoffel integrals. (We borrow code to calculate the nodes and weights for the quadrature from SC Toolbox [11], an existing package for computing Schwarz–Christoffel maps for various simply and doubly connected geometries).

The side-length conditions give $K_1 + \cdots + K_m$ real equations, but the calculation of A removes one from this count. The final side-length conditions then add up to $K_1 + \cdots + K_m - 3$ real equations. The *positions* of Γ_2 through Γ_m with respect to Γ_1 are fixed by requiring that

$$f(z_{1,j}) - f(z_{1,1}) = w_{1,j} - w_{1,1}$$

[1] "No singularity may lie closer to an integration sub-interval than one-half the length of that subinterval." [12].

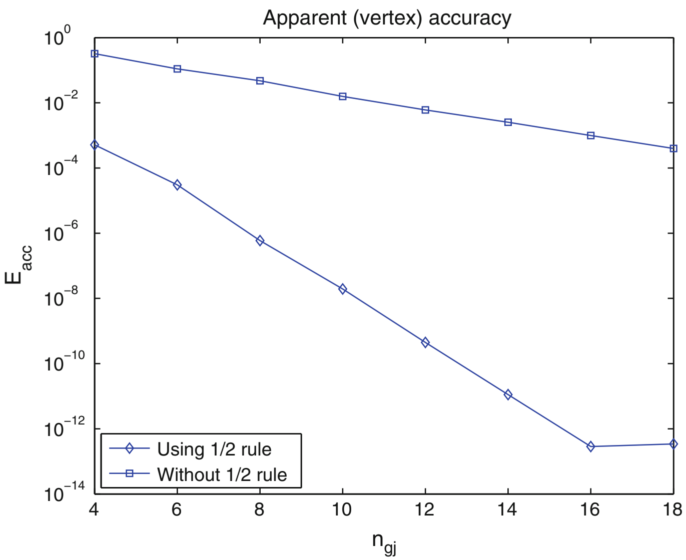

Fig. 5 Apparent (vertex) accuracy E_{acc} as a function of the number of quadrature points n_{gj}

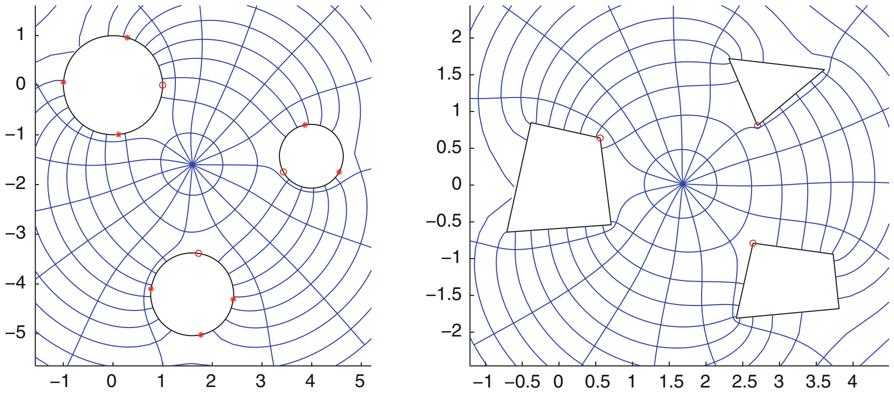

Fig. 6 Simple exterior map with $m = 3$. See Example 2. In this example the separation condition is satisfied, since $\Delta \approx 0.4078 < (m-1)^{-1/4} \approx 0.8409$

for $j = 2, \ldots, m$. These conditions give $2(m-1)$ real equations. Finally, the *orientations* of Γ_2 through Γ_m are given by the m real equations,

$$\arg(f(z_{2,j}) - f(z_{1,j})) = \arg(w_{2,j} - w_{1,j})$$

for $j = 2, \ldots, m$. (The orientation of Γ_1 is determined by the calculation of A). Therefore, the side-length, position, and orientation conditions give

$$K_1 + \cdots + K_m + 3m - 4$$

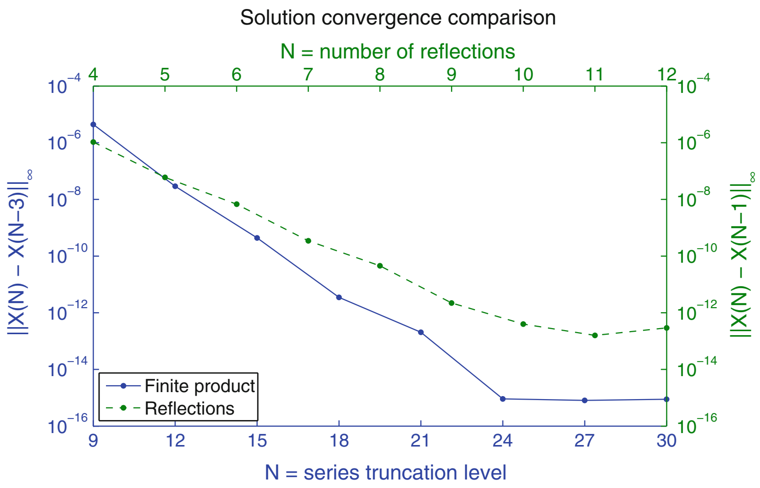

Fig. 7 Comparison of convergence of the solution to the parameter problem for both methods for Example 2

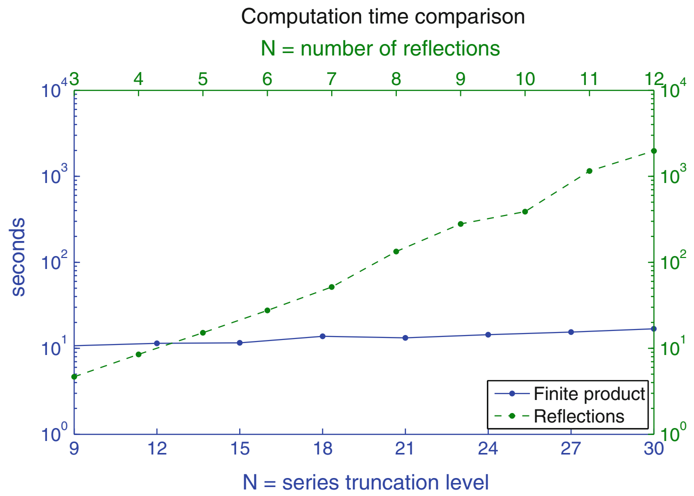

Fig. 8 Comparison of computation time to find the solution of the parameter problem for Example 2. Each method was started with the same initial guess

real equations. This is exactly what is needed. Other selections of conditions are possible and useful. In [10], the advantages of varying the numberings of the polygons and vertices and the locations of the integration paths between circles is discussed. We will not discuss these options here. However, we note that it is important that the resulting equations give a complete and independent set of conditions.

The constraints (53) on the $\theta_{k,j}$'s are difficult to enforce. As in [10], we therefore use a transformation to unconstrained variables similar to [12, p. 25]. Let $\phi_{k,j} := \theta_{k+1,j} - \theta_{k,j}$, $k = 1, \ldots, K_j$. Then the unconstrained variables are

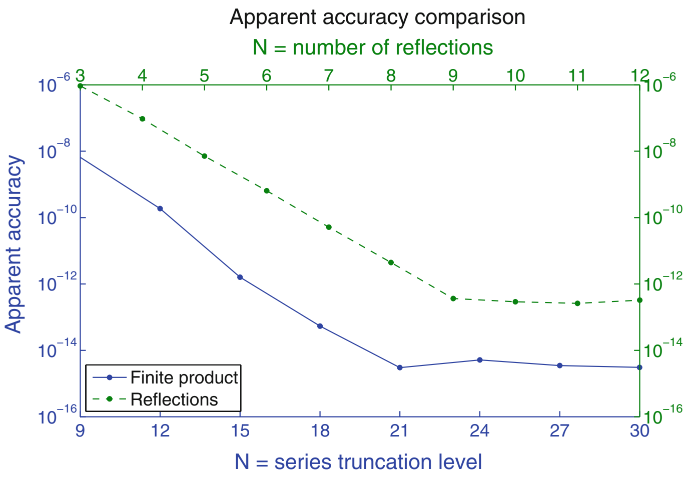

Fig. 9 Comparison of apparent accuracy E_{acc} for Example 2

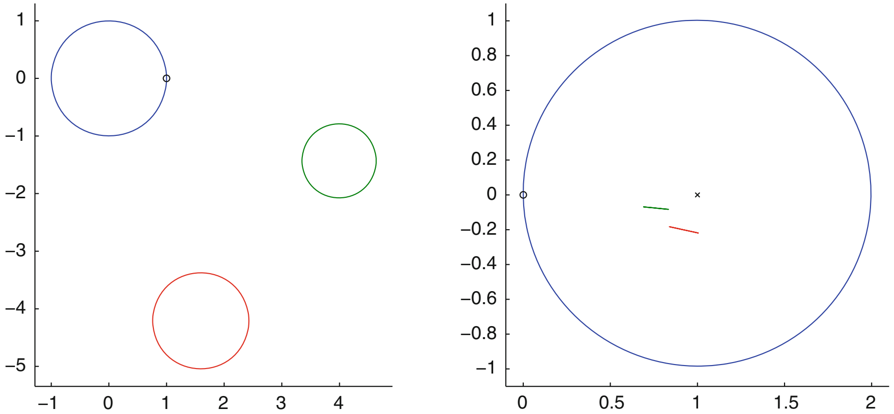

Fig. 10 The map $f_{z_{1,1}}$ for Example 2; i.e., the MCSC factor with $k = 1$, $j = 1$

$$\psi_{k,j} := \ln \frac{\phi_{k+1,j}}{\phi_{1,j}} \quad \text{for } k = 1, \ldots, K_j - 1. \tag{54}$$

Given $\theta_{1,j}$, the transformation (54) can be inverted by

$$\theta_{k,j} = \theta_{1,j} + 2\pi \frac{1 + \sum_{i=1}^{k-2} e^{\psi_{i,j}}}{1 + \sum_{i=1}^{K_j-1} e^{\psi_{i,j}}} \tag{55}$$

for $k = 2, \ldots, K_j$. Our unconstrained parameters are, therefore,

$$\theta_{1,j}, \psi_{1,j}, \psi_{2,j}, \ldots, \psi_{K_j-1,j},$$

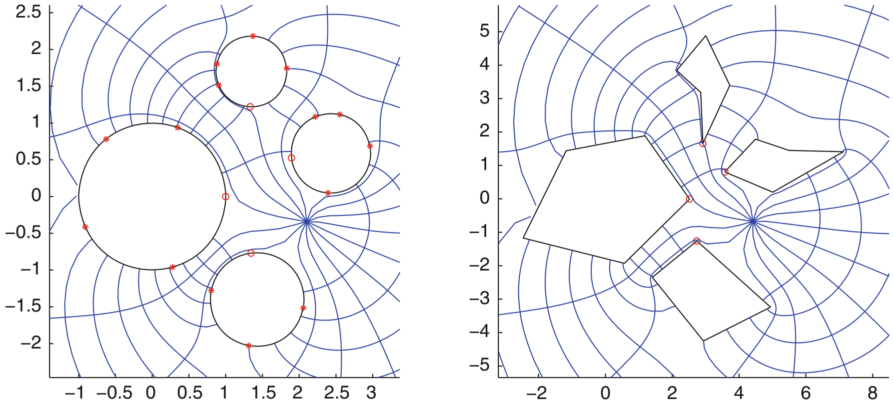

Fig. 11 Example 3 with $m = 4$ and higher vertex count

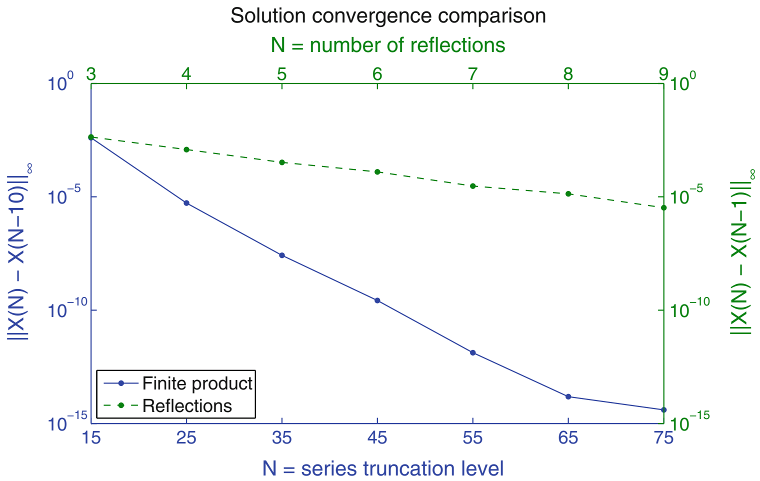

Fig. 12 Convergence comparison for the solution to the parameter problem for the 4-connected domain in Example 3. Note the slow convergence of the reflection method, since in this example we have $\Delta \approx 0.8164$ with $(m-1)^{-1/4} \approx 0.7598$

for $j = 1, \ldots, m$. (Recall that $\theta_{1,1} = 0$). The parameters are placed in a real vector X of length $n := K_1 + \cdots + K_m + 3m - 4$ and the non-linear equations form an $n \times n$ system $F(X) = 0$, where $F(X)$ is the objective function for our non-linear solver. As in [6,10], a homotopy search method [1, Program 3] is used here and found to be very effective. Convergence is almost always achieved even with a deliberately poor initial guess.

An estimate of the accuracy of the map, inspired by [11] is given. We attempt to calculate the images of the prevertices from the solution process, and then compare this result with known vertex values. The largest deviation from known values is then called the accuracy error, E_{acc}, or apparent (vertex) accuracy.

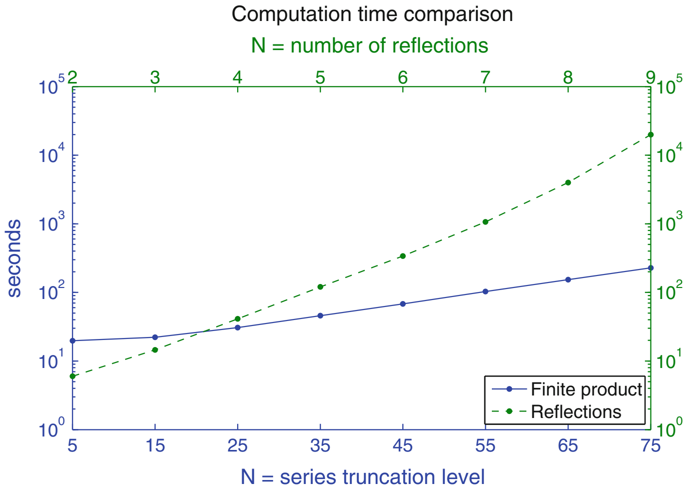

Fig. 13 Comparison of computation times for Example 3

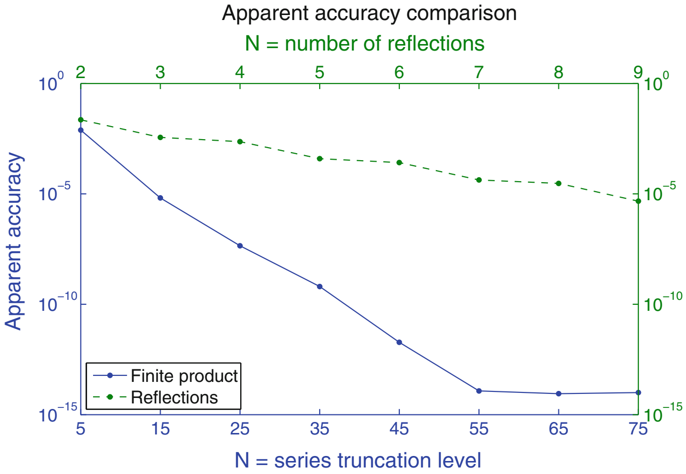

Fig. 14 Comparison of apparent accuracy E_{acc} for Example 3

Apparent accuracy is calculated by computing

$$E_{\mathrm{acc}} = \max_{j,k} \left| \left(A \int_{z_{k,j}}^{z_{k+1,j}} p(z)\,\mathrm{d}z + w_{k,j} \right) - w_{k+1,j} \right|, \tag{56}$$

where the integration path should be through the domain, away from the boundaries. In the simply connected circle map a similar calculation is done [11], but the integration path is a line from one prevertex to the origin, and then from the origin to the other

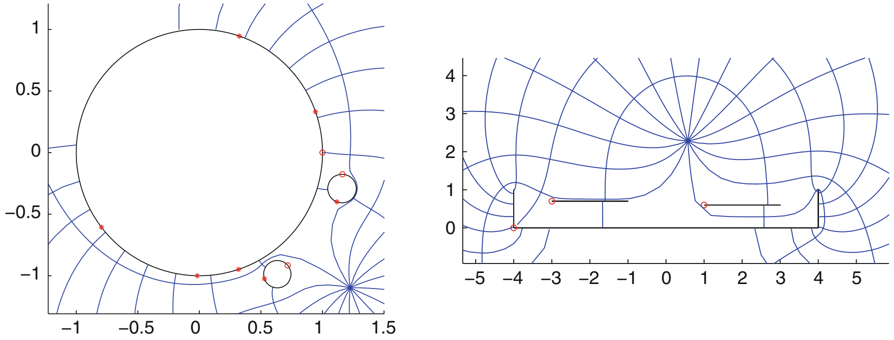

Fig. 15 For Example 4 with $m = 3$, the circles in the domain are very close to touching with $\Delta \approx 0.9474 > (m-1)^{-1/4} \approx 0.8409$

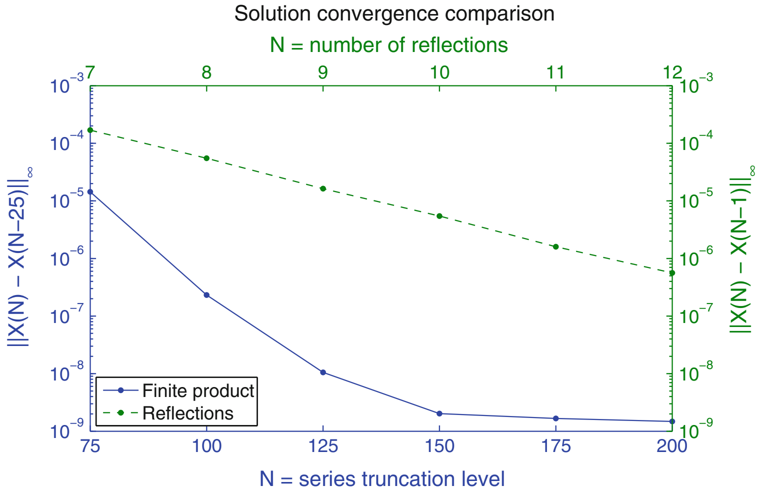

Fig. 16 Convergence for Example 4

prevertex. In the multiply connected case there is no convenient single point through which to integrate each of these (one might integrate through a singularity).

A simple solution to this consists of expanding the radius of each circle by adding 1/2 the distance to the closest circle. We then integrate out radially from a prevertex on the boundary to the associated point on the expanded circle, integrate along the arc of the expanded circle to the point associated with the next prevertex, and then radially inward from the associated point, to the prevertex on the boundary. In other words let c_j, r_j, $z_{k,j}$ and $z_{k+1,j}$ be the center and radius and two prevertices of a circle in question with $\theta_{k,j}$ and $\theta_{k+1,j}$ the angles of the prevertices. Set

$$\tilde{r}_j = r_j + \frac{1}{2} \min_{p \neq j} \{|c_j - c_p| - r_j - r_p\} \quad \text{for} \quad j, p \in \{1, \ldots . m\}. \tag{57}$$

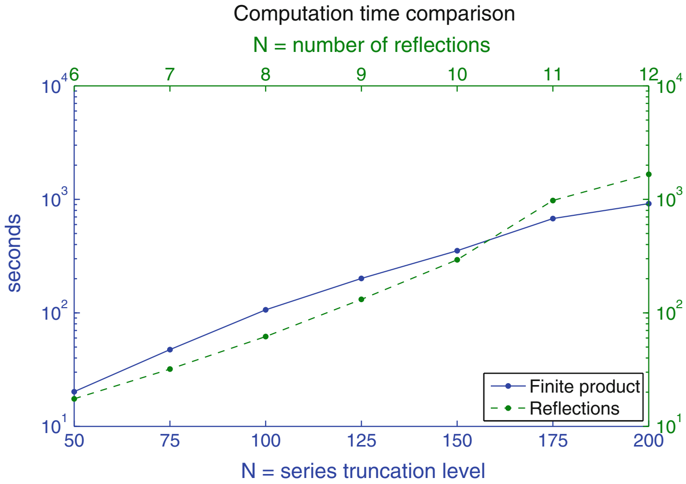

Fig. 17 Time comparison for Example 4

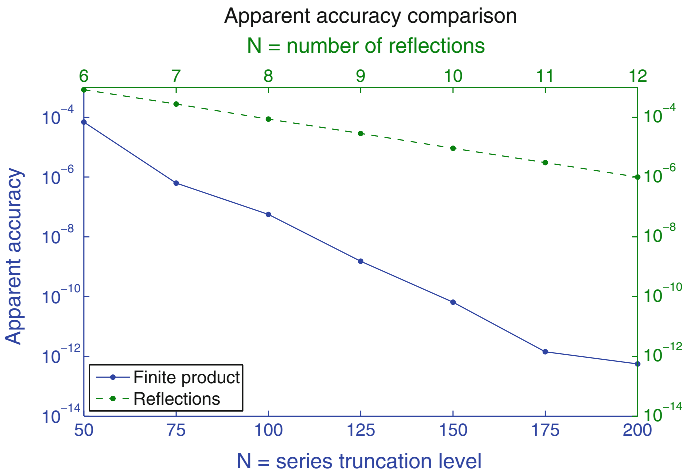

Fig. 18 Comparison of apparent accuracy E_{acc} for Example 4

Now set $\tilde{z}_{k,j} = c_j + \tilde{r}_j e^{i\theta_{k,j}}$ and $\tilde{z}_{k+1,j} = c_j + \tilde{r}_j e^{i\theta_{k+1,j}}$. We compute

$$\int_{z_{k,j}}^{z_{k+1,j}} p(z)\,\mathrm{d}z = \left(\int_{z_{k,j}}^{\tilde{z}_{k,j}} p(z)\,\mathrm{d}z + \int_{\tilde{z}_{k,j}}^{\tilde{z}_{k+1,j}} p(z)\,\mathrm{d}z + \int_{\tilde{z}_{k+1,j}}^{z_{k+1,j}} p(z)\,\mathrm{d}z \right) \tag{58}$$

where on the right-hand side of the equation, the first and last integrals are along radial lines, and the middle integral is along the arc of the expanded circle.

Figure 5 gives the relationship between E_{acc} and n_{gj}, the number of quadrature points in each compound integration interval, for the geometry shown in Fig. 4. The

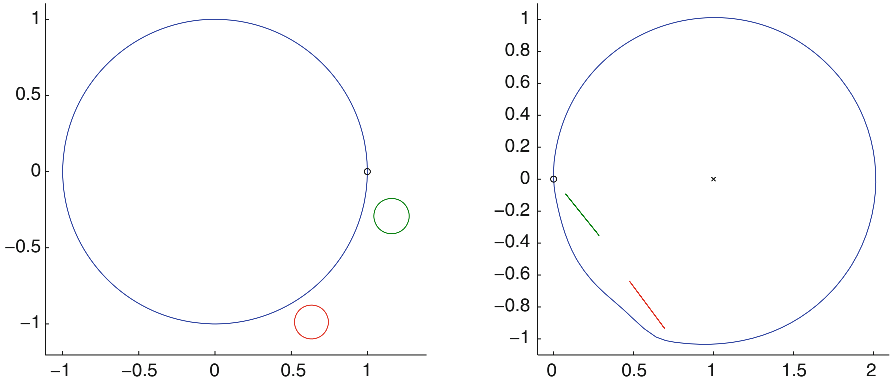

Fig. 19 The MCSC factor map $f_{z_{1,1}}$ for Example 4

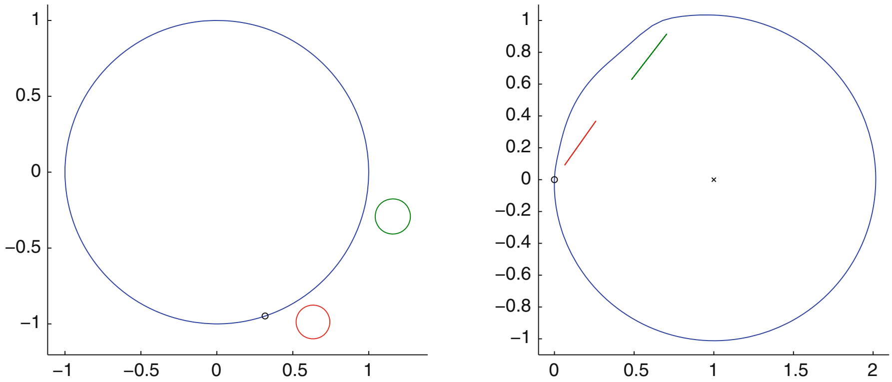

Fig. 20 The MCSC factor map $f_{z_{6,1}}$ for Example 4

re-entrant corners on the polygon were chosen to create singularities to ensure the one-half rule is necessary for accurate computation; the slits were chosen to ensure $\Delta << (m-1)^{-1/4}$.

5 Numerical Examples

Here we give numerical examples of the finite product computations using least squares, as well as comparisons with the reflection method. The examples below use these representations to evaluate the derivative of the MCSC transformation in solving the parameter problem as outlined in [9, 10].

Example 2 Our first example is shown in Fig. 6. It is clear from Figs. 7, 8, and 9 that the finite product method performs much better than the reflection method; one gets better convergence and accuracy for less computation time. The vectors $X(N)$ are the MCSC parameters after the solution process has finished at N levels of reflection or a series truncation level of N terms appropriately. We compare $\|X(N) - X(N-1)\|_\infty$

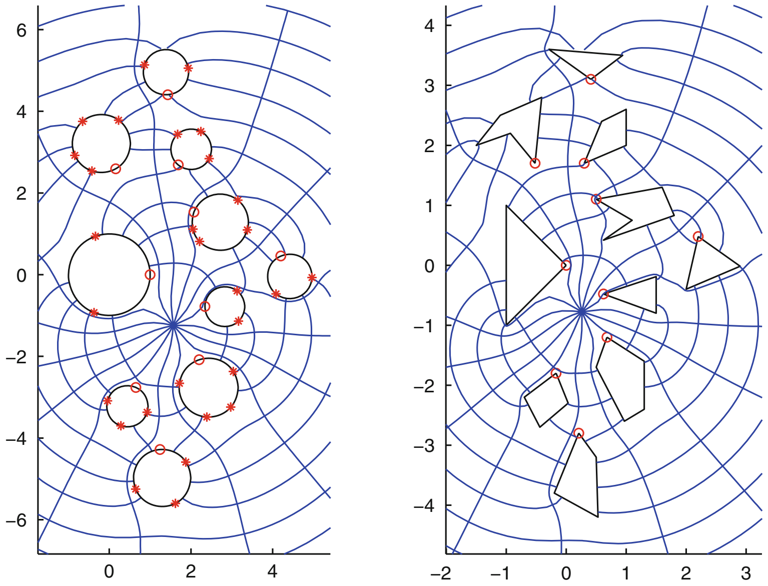

Fig. 21 Example 5 with high connectivity, $m = 10$. This took around 5 h to solve the parameter problem with the reflection method, and around 5 min using the finite product method

in the case of reflections and $\|X(N) - X(N-3)\|_\infty$ for the series. Figure 10 shows one of the slit maps in the finite product representation.

Example 3 The next example, see Figures 11, 12, 13, 14, is only slightly more complicated with four unbounded polygons ($m = 4$), but shows a more extreme example of the difference in time and accuracy of the two methods. This is due to the higher connectivity and higher vertex count. Note that for this example the separation condition is not satisfied, since $\Delta \approx 0.8164 > (m-1)^{-1/4} \approx 0.7598$.

Example 4 This example compares performance of the two methods in a domain with close to touching circles. See Fig. 15. Figures 16, 17, and 18 show the finite product method achieves better accuracy for approximately the same computation time. Even with $\Delta \approx 0.9474 > (m-1)^{-1/4} \approx 0.8409$, Figs. 19 and 20 show that, as in the reflection case, the separation condition is not necessary for convergence of the infinite series for the $f_{z_{k,j}}$'s.

Example 5 The last example involves high connectivity, $m = 10$; see Fig. 21. On the same hardware, the reflection method took just a little over 5 h to solve the parameter problem, while the finite product method took around 5 min to solve the same problem.

5.1 Polygonal Domain Vertices

In the interest of reproducibility, we list the vertices of the polygonal domains used in the above examples. Each polygonal domain is listed as a MATLAB cell array with vectors of vertices for each polygon as entries.

Example 2 $\{[0.56+0.64i,\ -0.38+0.85i,\ -0.71-0.64i,\ 0.71-0.54i],\ [2.70+0.81i,\ 3.61+1.57i,\ 2.31+1.72i],\ [2.64-0.79i,\ 2.41-1.81i,\ 3.81-1.68i,\ 3.73-0.94i]\}$

Example 3 $\{[2.52-0.007i,\ 1.19+1.89i,\ -1.17+1.44i,\ -2.46-1.17i,\ 0.57-1.93i],\ [2.74-1.26i,\ 1.41-2.35i,\ 2.94-4.25i,\ 4.94-3.24i],\ [3.57+0.80i,\ 5.01+0.2i,\ 7.12+1.41i,\ 5.5+1.45i,\ 4.49+1.79i][2.92+1.66i,\ 3.72+3.39i,\ 3.00+4.88i,\ 2.14+3.84i,\ 2.85+3.18i]\}$

Example 4 $\{[[-4,\ -4+1i,\ -4,\ 4,\ 4+1i,\ 4],\ [-3+0.7i,\ -1+0.7i],\ [1+0.6i,\ 3+0.6i]\}$

Example 5 $\{[0-1+1i-1-1i],\ [-.17-1.8i,\ -.7-2.2i,\ -.44-2.7i,\ .032-2.3i],\ [.21-2.8i,\ -.2-3.8i,\ .53-4.2i,\ .5-3.2i],\ [.68-1.2i,\ .5-1.7i,\ .97-2.6i,\ 1.3-2.4i,\ 1.3-1.6i],\ [.62-.48i,\ 1.5-.8i,\ 1.5-.19i],\ [2.2+.48i,\ 2-.4i,\ 2.9-.015i],\ [.5+1.1i,\ 1.1+.75i,\ .62+.42i,\ 1.8+.83i,\ 1.6+1.3i],\ [.3+1.7i,\ 1+2i,\ 1+2.6i,\ .59+2.4i],\ [.41+3.1i,\ .94+3.5i,\ -.29+3.6i],\ [-.52+1.7i,\ -.41+2.8i,\ -1.1+2.5i,\ -1.5+2i,\ -.93+2.2i]\}$

References

1. Allgower, E.L., Georg, K.: Numerical Continuation Methods: An Introduction. Springer, New York (1990)
2. Crowdy, D.: Schwarz–Christoffel mapping to unbounded multiply connected polygonal regions. Math. Proc. Camb. Phil. Soc. **142**, 319–339 (2007)
3. Crowdy, D.: The Schottky–Klein prime function on the Schottky double of planar domains. Comput. Methods Funct. Theory **10**, 501–517 (2010)
4. Crowdy, D., Marshall, J.: Computing the Schottky–Klein prime function on the Schottky double of planar domains. Comput. Methods Funct. Theory **7**, 293–308 (2007)
5. DeLillo, T.K.: Schwarz–Christoffel mapping of bounded, multiply connected domains. Comput. Methods Funct. Theory **6**, 275–300 (2006)
6. DeLillo, T.K., Driscoll, T.A., Elcrat, A.R., Pfaltzgraff, J.A.: Computation of multiply connected Schwarz–Christoffel maps for exterior domains. Comput. Methods Funct. Theory **6**, 301–315 (2006)
7. DeLillo, T.K., Driscoll, T.A., Elcrat, A.R., Pfaltzgraff, J.A.: Radial and circular slit maps of unbounded multiply connected circle domains. Proc. R. Soc. A. **464**, 1719–1737 (2008)
8. DeLillo, T.K., Elcrat, A.R., Pfaltzgraff, J.A.: Schwarz–Christoffel mapping of multiply connected domains. J. d'Anal. Math. **94**, 17–47 (2004)
9. DeLillo, T.K., Kropf, E.H.: Slit maps and Schwarz–Christoffel maps for multiply connected domains. Electron. Trans. Numer. Anal. **36**, 195–223 (2010)
10. DeLillo, T.K., Kropf, E.H.: Numerical computation of the Schwarz–Christoffel transformation for multiply connected domains. SIAM J. Sci. Comput. **33**, 1369–1394 (2011)
11. Driscoll, T.: A MATLAB toolbox for Schwarz–Christoffel mapping. ACM Trans. Math. Softw. **22**, 168–186 (1996)
12. Driscoll, T., Trefethen, L.: Schwarz–Christoffel Mapping. Cambridge University Press, Cambridge (2002)
13. Finn, M.D., Cox, S.M., Byrne, H.M.: Topological chaos in inviscid and viscous mixers. J. Fluid Mech. **493**, 345–361 (2003)
14. Henrici, P.: Applied and Computational Complex Analysis, vol. III. Wiley, New York (1986)
15. Kropf, E.: Numerical computation of Schwarz-Christoffel transformations and slit maps for multiply connected domains, PhD Dissertation, Department of Mathematics, Statistics, and Physics, Wichita State University (2012)
16. Mityushev, V.: Schwarz–Christoffel formula for multiply connected domains. Comput. Methods Funct. Theory **12**, 449–463 (2012)

17. Trefethen, L.N.: Numerical computation of the Schwarz–Christoffel transformation. SIAM J. Stat. Comput. **33**, 82–102 (1980)
18. Trefethen, L.N.: Ten digit algorithms, Report No. 05/13, Oxford University Computing Laboratory (2005)